Electronic Supplementary Material (ESI) for ChemComm.
This journal is © The Royal Society of Chemistry 2020

Janus and core@shell gold nanorod@$Cu_{2-x}S$ supraparticles: reactive sites regulation fabrication, optical/catalytic synergetic effects and enhanced photothermal efficiency/photostability

Biao Wang, Ruirui Li, Ge Guo and Yunsheng Xia*

Key Laboratory of Functional Molecular Solids, Ministry of Education, College of Chemistry and Materials Science, Anhui Normal University, Wuhu 241000, China.

Email: xiayuns@mail.ahnu.edu.cn

Materials

$HAuCl_4 \cdot 3H_2O$, bovine serum albumin (BSA), cell counting kit-8 (CCK-8) were obtained from Sigma-Aldrich (St. Louis, MO, USA). Hexadecyl trimethylammonium Bromide (CTAB), terephthalic acid, ascorbic acid (AA), $NaBH_4$, $AgNO_3$, HCl, 3,3',5,5'-tetramethylbenzidine (TMB), NaH_2PO_4, Na_2HPO_4, CH_3COOH, $CuSO_4 \cdot 5H_2O$, NaOH, CH_3COONa and H_2O_2 were acquired from Shanghai Reagent Company. Dulbecco's Modified Eagle Medium (DMEM), fetal bovine serum (FBS), 0.05% trypsin-EDTA and penicillin-streptomycin were purchased from Gibco Invitrogen Co. (New York, USA). Calcein-AM/PI Double Stain Kit was purchased from Shanghai Yeasen BioTechnologies Co., Ltd. All chemicals were used as received. All solutions were prepared in Milli-Q water (Millipore, USA, resistivity >18 MΩ·cm).

Characterization methods and instruments

Extinction spectra were recorded with a U-2910 spectrometer (Hitachi, Japan). Fluorescence spectra were recorded with a Hitachi F-4600 fluorescence spectrophotometer. Transmission

electron microscopy (TEM) was carried out on a HT-7800 electron microscope (Hitachi, Japan) under the accelerating voltage of 100 kV. High-resolution (HR) TEM images were captured by a Tecnai G2 20ST TEM (FEI, USA) under the accelerating voltage of 200 kV. The morphology and chemical elements were analyzed by transmission electron microscopy (TEM, FEI Talos F200S) equipped with energy dispersive X-ray spectroscopy (EDS, FEI Talos F200S). X-ray powder diffraction (XRD) patterns were characterized with a Shimadzu XRD-6000 X-ray diffractometer equipped with Cu Kα1 radiation (λ = 0.15406 nm). The thicknesses of various samples were detected by a Dimension Icon PT atomic force microscopy (AFM, Bruker, Switzerland). The hydrodynamic sizes and ξ-potential values were measured at 25 °C using a Zetasizer Nano ZS instrument (Malvern, UK) with 633 nm laser wavelength and a measurement angle of 173° (backscatter detection). X-ray photoelectron spectroscopy (XPS) measurements were performed by an ESCALAB 250Xi XPS (Thermo Fisher Scientific, USA) equipped with ultra-high vacuum (1×10^{-9} Pa or lower) and monochromatic Al Kα (1486.6 eV) X-ray radiation (15 kV and 12 mA). An 808 nm laser with 0.75 W cm^{-2} (CNI, China) was used for in vitro photothermal irradiation. Fluorescence microscopy images were implemented on an automated inverted optical microscope (Olympus IX83, Japan). The amounts of Au and Cu were measured by inductively coupled plasma optical emission spectra (ICP-OES) analysis (Agilent 720ES).

Synthesis and purification of GNRs

GNRs were prepared in aqueous solutions using a seeded growth method.[s1] Specifically, the gold seed solution was first obtained by the addition of $HAuCl_4$ solution (0.01 M, 0.25 mL) into CTAB solution (0.1 M, 9.75 mL) in a 50 mL erlenmeyer flask. A freshly prepared, ice-cold $NaBH_4$

solution (0.01 M, 0.6 mL) was then introduced quickly into the mixture solution, followed by rapid inversion for 2 min. The resultant seed solution was kept in a 30 °C water bath for 2 h before use. To grow GNRs, $HAuCl_4$ (0.01 M, 7.5 mL) and $AgNO_3$ (0.01 M, 1.2 mL) were first mixed with CTAB (0.1 M, 150 mL) in a 250 mL plastic tube. Then, HCl (1.0 M, 3 mL) was added for pH adjustment of the growth solution, followed by the addition of ascorbic acid (0.1 M, 1.2 mL). After the growth solution was mixed by inversion, the Au seed solution (0.21 mL) was rapidly injected. The resultant solution was gently mixed for 10 s and left undisturbed 12 h in 30 °C water bath. For purification of the GNRs, 5 mL of the GNRs solution was collected by centrifugation at 8000 rpm for 10 min, and it was further washed two times by water. The concentration of the GNRs was estimated by Lambert-Beer law.[S2]

Synthesis of the Janus GNR@$Cu_{2-x}S$ SPs

First, the purified GNRs (7.5 nM, 1.0 mL) were dispersed in CTAB solution (1.0 mM, 5.0 mL). Then, BSA (80 mg mL^{-1}, 2.5 mL) and $CuSO_4 \cdot 5H_2O$ (1.5 mM, 1.0 mL) were added into the above solution under continuous stirring, followed by adjusting the pH to 12 with 1 M NaOH. The resulting solution was left undisturbed 6 h in 80 °C water bath. For purification of the Janus SPs, the original solution was centrifuged at 7000 rpm for 10 min. The obtained precipitate was further washed by water and then redispersed in water.

Synthesis of the core@shell GNR@$Cu_{2-x}S$ SPs

First, the as-prepared purified GNRs (7.5 nM, 1.0 mL) were dispersed in CTAB solution (20.0 mM, 5.0 mL). Then, BSA (240 mg mL^{-1}, 2.5 mL) and $CuSO_4 \cdot 5H_2O$ (20 mM, 1.0 mL) were added into the

above solution under continuous stirring, followed by adjusting the pH to 12 with 1 M NaOH. The resulting solution was left undisturbed 12 h in 60 °C water bath. For purification of the core@shell SPs, the original solution was centrifuged at 7000 rpm for 10 min (These processes were repeated two times to modulate the diameters of the decorated $Cu_{2-x}S$).The obtained precipitate was further washed by water and then redispersed in water.

Photothermal study

To study the photothermal performances of Janus and core@shell SPs, 1 mL aqueous dispersion of Janus and core@shell SPs with different concentrations (0 − 200 μg mL^{-1}) were irradiated with an 808 nm NIR laser at a power density of 0.75 W cm^{-2}, respectively. An IR thermal camera (Fotric 226s) was used record the temperature of the solution at each time point. The photothermal conversion efficiency of GNRs was determined at the same conditions as those for the GNRs@$Cu_{2-x}S$ SPs.

To compare the photothermal stability, GNRs, Janus and core@shell SPs with same extinction (~ 0.4) at 808 nm were chosen. The samples (1 mL) were irradiated with an 808 nm laser with an output of 0.75 W cm^{-2} for 10 min, followed by naturally cooling to room temperature without irradiation, and this cycle was repeated six times.

Calculation of the photothermal conversion efficiency

The photothermal conversion efficiency (η) is calcuted by the following equations,[S3] Detailed calculation was given as following:

$$\eta = \frac{hS(T_{max} - T_{surr}) - Q_{dis}}{I(1 - 10^{-A_{808\ nm}})} \qquad (1)$$

where h is the heat transfer coefficient, S is the irradiated area, Q_{dis} is the baseline energy input from the light absorption by the solvent (which is measured independently to be 22 mW using pure water), T_{max} and T_{surr} are the highest temperature of system and the temperature of surrounding (the value of $T_{max} - T_{surr}$ equals 25.6, 38.3 and 36.6 °C, using the data of GNRs, GNRs@$Cu_{2-x}S$ Janus and Core@Shell SPs colloid system, respectively.), I is the incident laser power (0.75 W cm^{-2}), A_{808nm} is the absorption of GNRs, GNRs@$Cu_{2-x}S$ Janus and Core@Shell SPs at 808nm (A_{808nm} = 0.4).

The value of hS is calculated by using the following equation (2) to (4):

$$hS = \frac{\sum m_i C_{P,i}}{\tau_s} \qquad (2)$$

$$t = -\tau_s \ln \theta \qquad (3)$$

$$\theta = \frac{T - T_{surr}}{T_{max} - T_{surr}} \qquad (4)$$

where m and C_p are the mass (1.0 g) of sample and the thermal capacity (4.2 J g^{-1}) of sample and t is cooling time after irradiation. τ_s is the sample system time constant, θ is the dimensionless driving force temperature, T is the temperature at the cooling time (t) after turning off the light source, and τ_s can be determined by linear fitting cooling time (t) to negative natural logarithm of temperature (−ln θ).

Terephthalic acid probing technique

H_2O_2 (200 μL, 10 mM), terephthalic acid (200 μL, 5 mM) and Janus SPs (1 ml, 100 μg mL^{-1}) were incubated in acetate buffer solutions (0.1 M, pH 4.5) at 37 °C. The fluorescence spectra under the excitation wavelength of 315 nm were recorded after 2 h using a spectrofluorophotometer.

Peroxidase-like activity assay

Measurements were carried out in 2 mL AcOH buffer solution (0.1 M, pH 4.5) containing different concentrations of the Janus SPs (0, 6.25, 12.5, 25, 50, 75 and 150 μg mL^{-1}), H_2O_2 (1 mM),

and TMB (0.5 mM) at 37 °C for 30 min. The absorbance spectra were observed using a UV−Vis spectrometer. In addition, peroxidase-like activity of the Janus SPs (50 μg mL^{-1}) was determined while varying the pH from 3.5 to 7.5 and the temperature from 25 to 75 °C.

In vitro cytotoxicity and photothermal therapy of cells

The cytotoxicity of the Janus SPs incubated with HUVEC, HepG2 and HeLa cells were evaluated by using the CCK-8 assay. Cells were seeded at a density of 1×10^4 cells per well in 96−well plates and incubated with the DEME medium supplemented with 10% FBS, 100 U mL^{-1} penicillin, and 100 μg mL^{-1} streptomycin in a 5% CO_2 environment at 37 °C for 24 h. After incubation, the cell medium was removed, and cells were washed with PBS. The Janus SPs solutions were then diluted appropriately in fresh culture media and added to 96−well plates (200 μL) at concentrations of 0, 6.25, 12.5, 25, 50, 100, 200 μg mL^{-1}. After incubation for 24 h, the cell medium was replaced with fresh culture media to remove free NPs in the solution. Subsequently, Cell cytotoxicity was evaluated by the CCK-8 colorimetric procedure.

To evaluate the *in vitro* photothermal ablation efficiency, 200 μL solution containing different concentrations of the Janus SPs was added into the wells containing HepG2 and HeLa cells. After incubation for 24 h, cells were followed by a 5 or 10 min irradiation (808 nm, 0.75 W cm^{-2}). Cell viability after photothermal treatment was then evaluated by CCK-8 assays. Calcein-AM/PI Double Stain Kit was used for live and dead cell staining.

Finite-difference time domain (FDTD) simulation

The FDTD simulation was performed by the Lumerical software package 8.6.0 (Lumerical Solutions, Inc.). A total-field/scattered field (TFSF) source (400-1600 nm) was used as an incident field into the simulation region. To imitate the dielectric circumstance in the experiment, the background dielectric constant was fixed at 1.33 (water). The mesh of simulation region was set to be 1.0 nm in each direction. The dielectric function of Au was taken from Johnson and Christy's data,[S4] while that of the $Cu_{2-x}S$ nanocrystal is expressed as a function of the frequency of light, ω, by the Drude model:

$$\varepsilon(\omega) = 1 - \frac{\omega_p^2}{\omega^2 + i\gamma\omega}$$

Here ω_p is the bulk plasma oscillation frequency associated with the free carriers and γ is their bulk collision frequency. ω_p and γ were deduced by the experimental absorption spectra as $4*10^{15}$ rds s^{-1} and $9*10^{14}$ rds s^{-1}, respectively.

Supplementary data

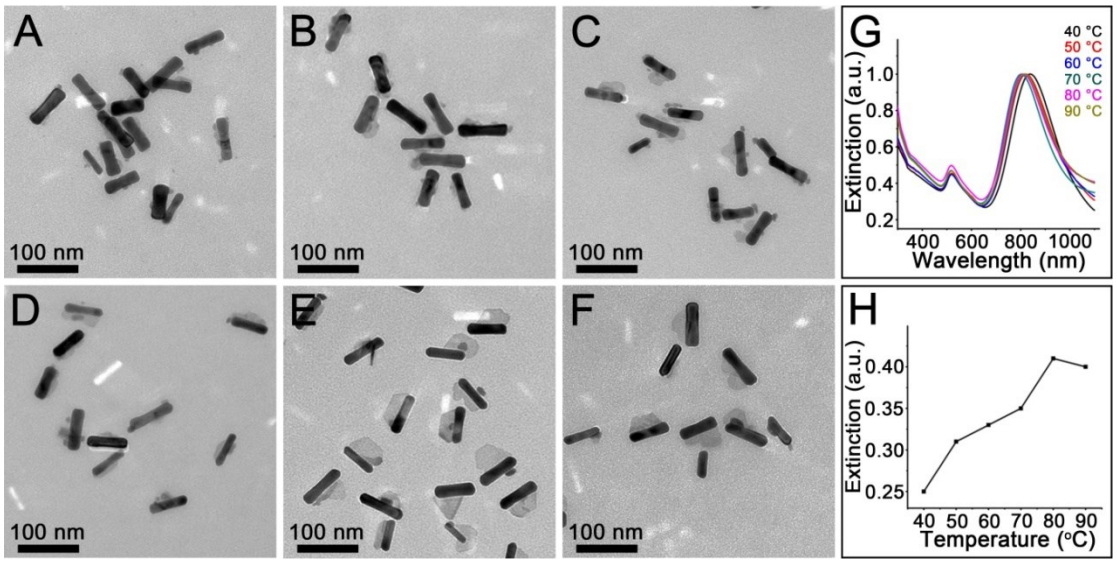

Fig. S1 The Janus SPs were fabricated at different reaction temperature. TEM images of the products obtained at (A) 40, (B) 50, (C) 60, (D) 70, (E) 80 and (F) 90 °C. (G) Extinction spectra, (H) the line chart of temperature-dependent extinction at 1100 nm.

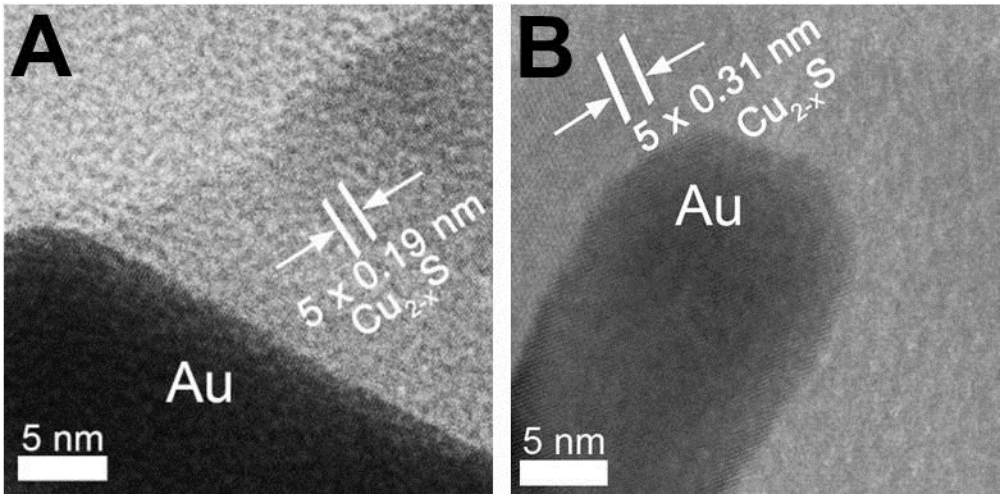

Fig. S2 HRTEM images of the Janus SPs (A) and the core@shell SPs (B). In terms of the core@shell products, the GNRs are well capped by a rather thicker $Cu_{2-x}S$ layer, which causes the passthrough difficulties of the electron beam during TEM measurements. As a result, the lattice fringes of the gold cores are difficult to be observed in the HRTEM image.

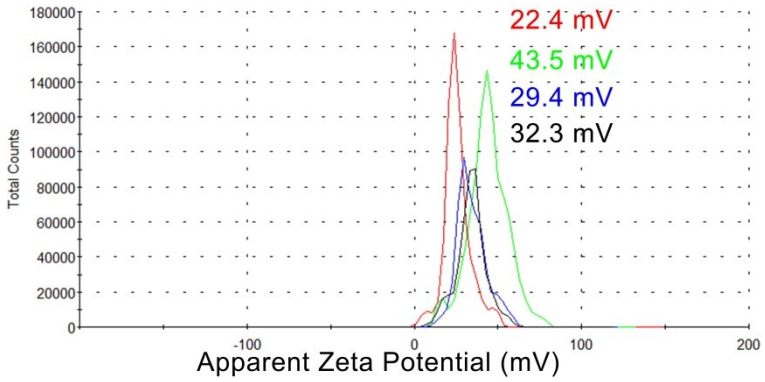

Fig. S3 Core@shell SPs' ξ-potential values of GNRs (red curve), (GNRs + CTAB (10 mM)) (green curve), (GNRs + CTAB (10 mM) + BSA (60 mg mL^{-1})) (blue curve) and (GNRs + CTAB (10 mM) + BSA (60 mg mL^{-1}) + Cu^{2+} (2 mM)) (black curve).

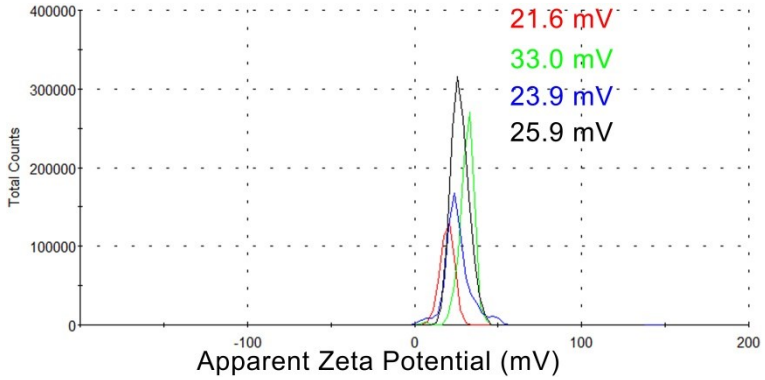

Fig. S4 Janus SPs' ξ-potential values of GNRs (red curve), (GNRs + CTAB (0.5 mM)) (green curve), (GNRs + CTAB (0.5 mM) + BSA (20 mg mL^{-1})) (blue curve) and (GNRs + CTAB (0.5 mM) + BSA (20 mg mL^{-1}) + Cu^{2+} (0.15 mM)) (black curve).

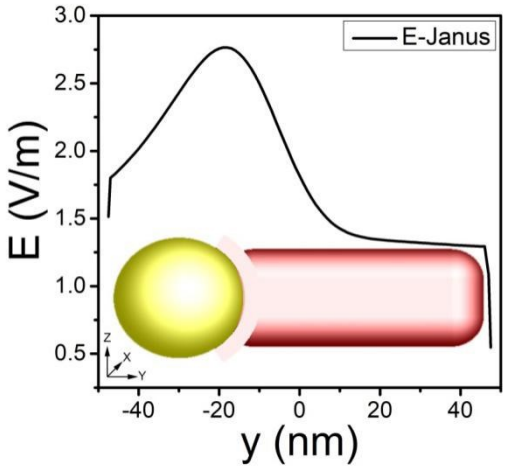

Fig. S5 The electric field density curve of the Janus SP irradiated with 808 nm laser along the longitudinal direction.

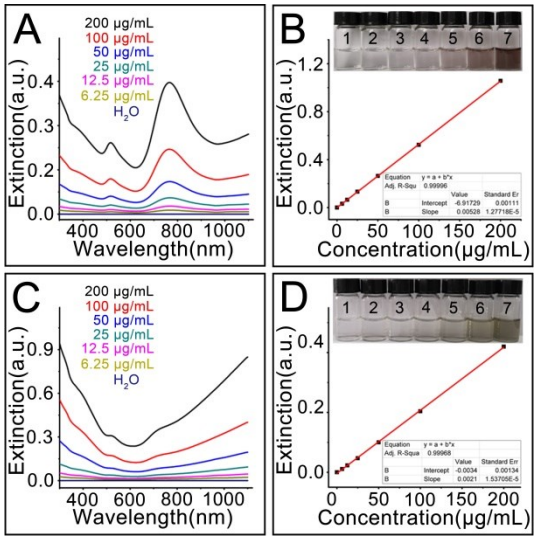

Fig. S6 Concentration dependent (A) extinction spectra and (B) extinction (the inset is the corresponding photo images) of the Janus SPs. Concentration dependent (C) extinction spectra and (D) extinction (the inset is the corresponding photo images) of the core@shell SPs.

The extinction coefficients of the Janus and core@shell SPs at 808 nm are 5.28 and 2.11 L g^{-1} cm^{-1}, respectively, which are comparable to that of other NIR nanomaterials ($Cu_{2-x}S$, $Cu_{2-x}Se$ NPs, etc.) on the whole.

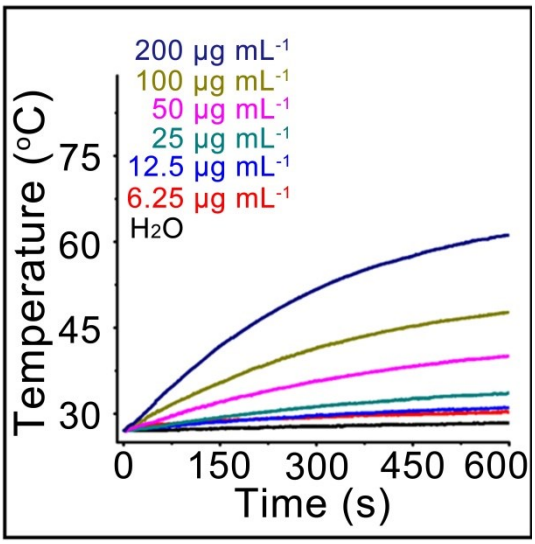

Fig. S7 Photothermal effects of core@shell SPs at different concentrations (0.75 W cm^{-2} 808 nm laser, 10 min irradiation).

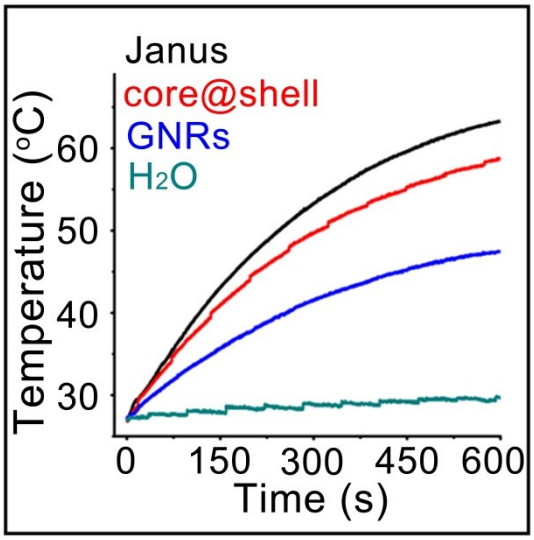

Fig. S8 Temperature profiles of four solutions (extinction value at 808 nm is 0.4).

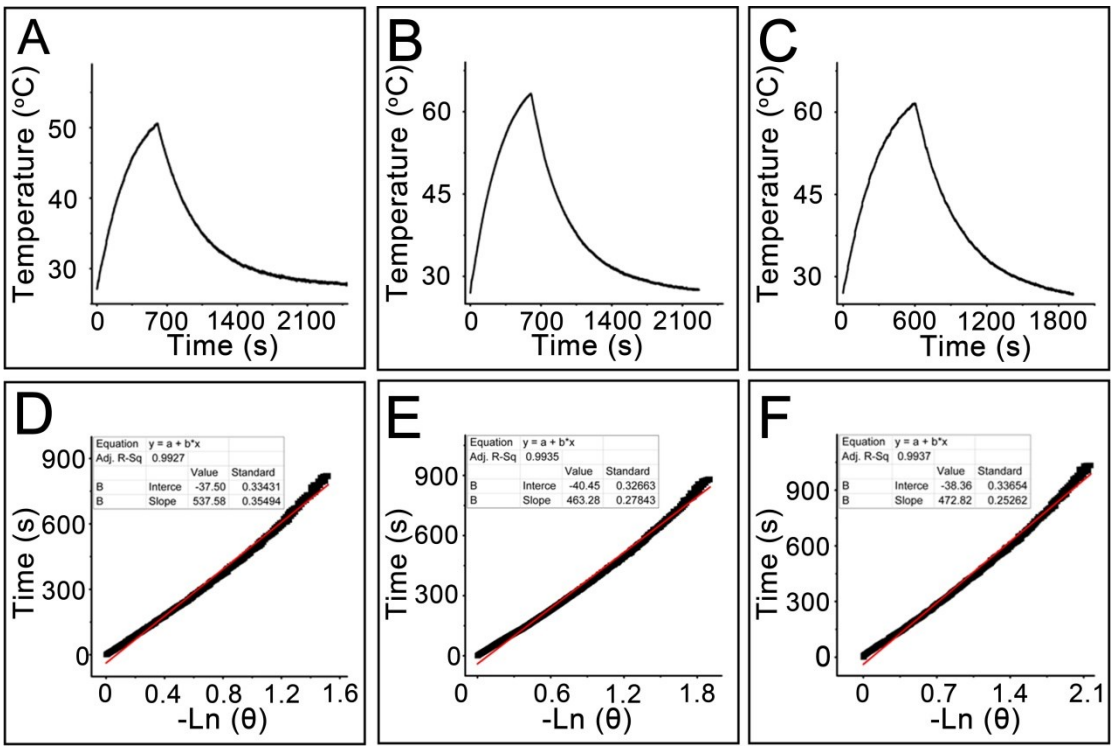

Fig. S9 The photothermal profile of AuNRs (A), Janus SPs (B) and core@shell SPs (C) aqueous solution (Extinction at 808 nm is 0.4) for 10 min with an NIR laser (808 nm, 0.75 W cm^{-2}) and then the laser was shut off. (D), (E) and (F) Linear time data versus −lnθ obtained from the cooling period of (A), (B) and (C), respectively. The photothermal conversion efficiency of GNRs, Janus and core@shell SPs is 35.5%, 66.4% and 61.2%, respectively.

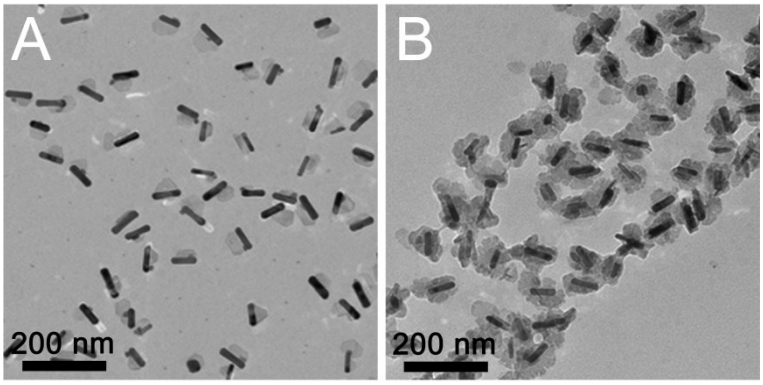

Fig. S10 The Janus (A) and core@shell (B) SPs before over 6 cycles of irradiation/cooling.

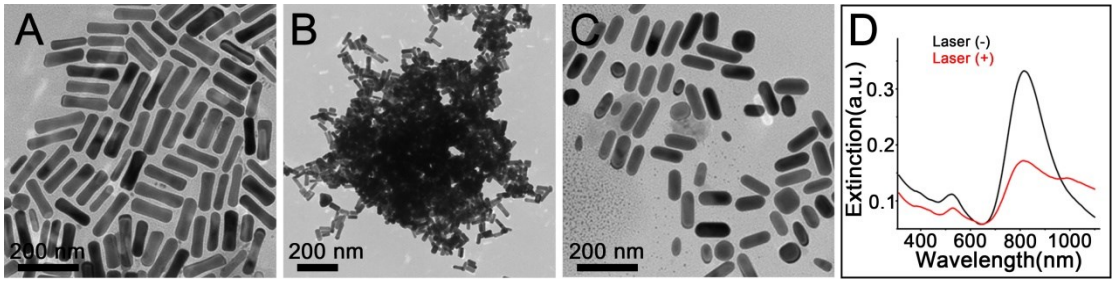

Fig. S11 TEM images of before cycles (A) and after cycles (B, C), extinction spectra (D) of GNRs before and after over 6 cycles of irradiation/cooling.

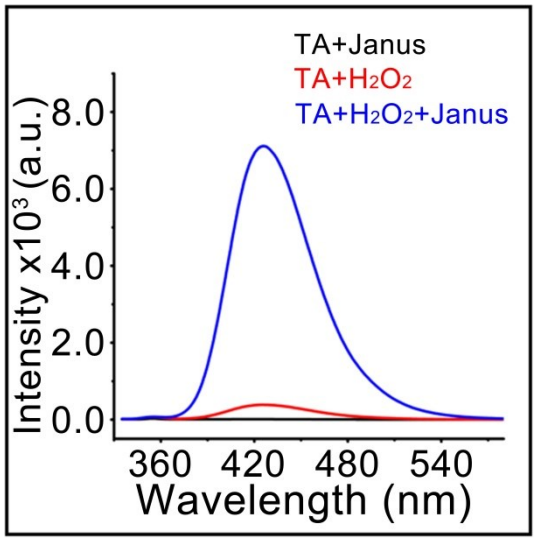

Fig. S12 Fluorescence spectra of three TA related systems of the Janus SPs. The distinct fluorescence enhancement (blue cyrve) indicates that •OH substances are well produced by the catalysis the Janus SPs.

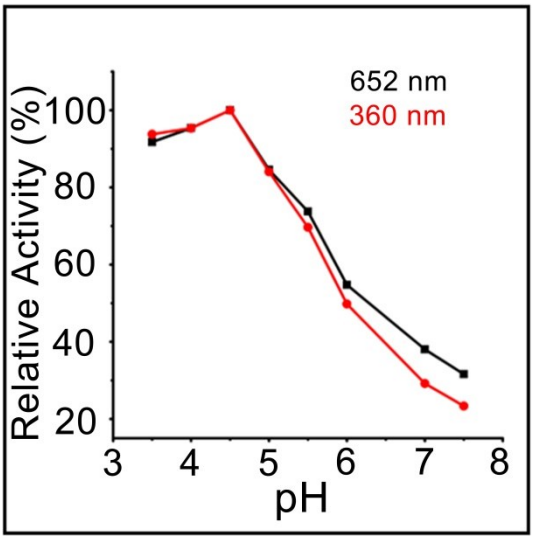

Fig. S13 pH *vs*. peroxidase-like activity of the Janus SPs. Even if the pH value is increased to 6, the activity is still rather obvious. This result indicates that the SPs can probably work at tumor sites, where the conditions are only weakly acidic.

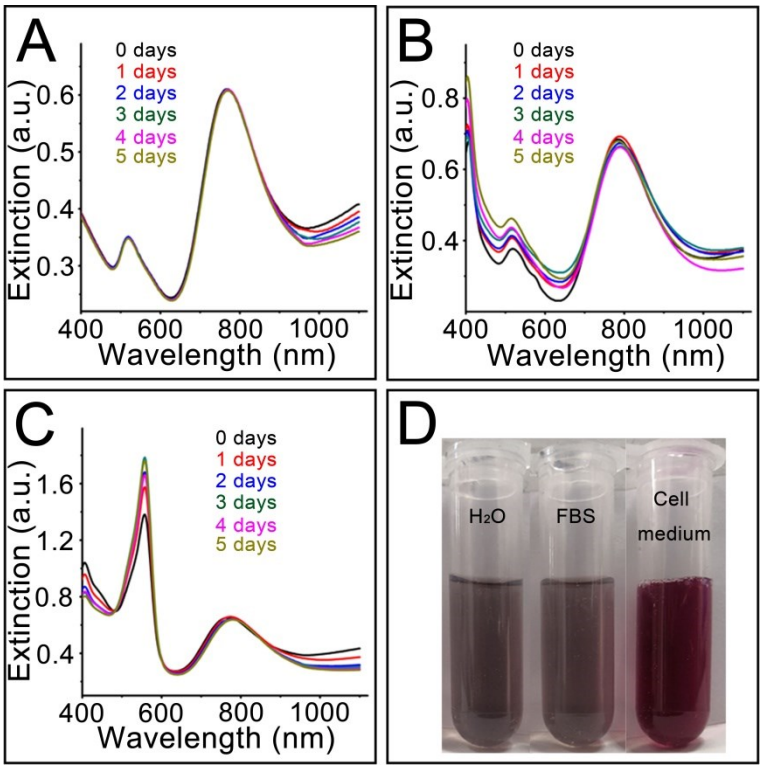

Fig. S14 The stability of the Janus SPs in different mediums.

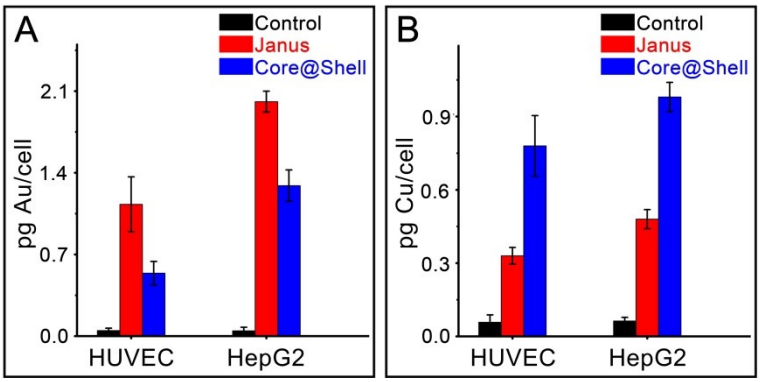

Fig. S15 Cell uptake after incubation with 24 h of the Janus and core@shell SPs (50 μg mL^{-1}).

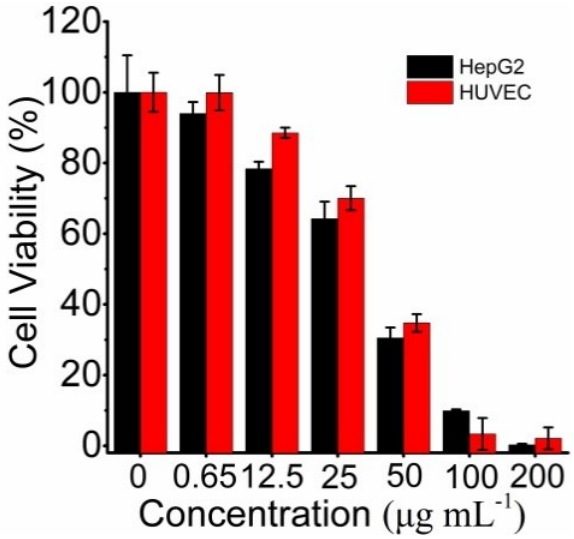

Fig. S16 Cell viability of HepG2 and HUVEC cells after incubation with various concentrations of the Janus SPs for 24 h and then irradiation with an 808 nm laser (0.75 W cm^{-2}, 10 min). The cell viability of the normal cells is some higher than that of tumor cells, which probably due to their lower cell uptake (Fig. S15). However, most of the normal cells can also be killed by the photothermal effects as the concentration of the used SPs reach 100 μg mL^{-1}. These results indicate that a target modification is probably essential for the further applications.

Table S1 The results of ICP-OES elemental analysis of the Janus SPs and core@shell SPs.

Samples	Extinction at 808 nm	Concentrations (μg·mL^{-1})		The mass ratios of Cu and Au
		Cu	Au	
Janus SPs	1	3.9	36.7	0.106
	0.6	2.3	22.3	0.103
	0.3	1.1	11.5	0.096
core@shell	1	31.2	24.9	1.253
SPs	0.6	18.8	14.6	1.288
	0.3	9.2	7.6	1.211

References:

S1 *(a)* B. Nikoobakht and M. A. El-Sayed, *Chem. Mater*., 2003, **15***,* 1957. *(b)* L. Lu and Y. Xia, *Anal. Chem*., 2015, **87**, 8584. *(C)* H. Zhu, Y. Wang, C. Chen, M. Ma, J. Zeng, S. Li, Y. Xia and M. Gao, *ACS Nano*, 2017, **11**, 8273.

S2 C. J. Orendorff and C. J. Murphy, *J. Phys. Chem. B*, 2006, **110**, 3990.

S3 *(a)* D. K. Roper, W. Ahn and M. Hoepfner, *J. Phys. Chem. C*, 2007, **111**, 3636. *(b)* Y. Liu, K. Ai, J. Liu, M. Dong, Y. He and L. Lu, *Adv. Mater*., 2013, **25**, 1353.

S4 P. B. Johnson and R. W. Christy, *Phys. Rev. B*, 1972, **6**, 4370.